Performance analysis of double-effect absorption heat pump cycle using NH_3/ILs pairs

Wang, Meng; Infante Ferreira, Carlos

Publication date
2017

Document Version
Final published version

Published in
Proceedings 12th IEA Heat Pump Conference

12th IEA Heat Pump Conference 2017

Performance analysis of double-effect absorption heat pump cycle using NH_3/ILs pairs

Meng Wang[a], Carlos A. Infante Ferreira[a]

Delft University of Technology, Process and Energy Department
Leeghwaterstraat 39, 2628 CB Delft, The Netherlands
M.Wang-2@tudelft.nl

Abstract

Ionic liquids (ILs), as novel absorbents, draw considerable attention for their potential roles in replacing H_2O or LiBr aqueous solutions in conventional NH_3/H_2O or H_2O/LiBr absorption chiller or heat pump cycles. In this paper, NH_3/IL working pairs are proposed for implementation in parallel double effect heat pump systems. To investigate their performance, a property-prediction method, based on experimental heat capacities and the non-random two-liquid (NRTL) activity coefficient model for the vapor pressure, was used to estimate the thermodynamic properties for the proposed NH_3/IL mixtures. Then, parallel configuration double-effect absorption heat pump cycles driven by a high-temperature heat source were analyzed by means of evaluation of the thermodynamic operating limits and performance simulations with the aforementioned properties. The ILs investigated include [Mmim][DMP], [Emim][BF_4], [Hmim][BF_4], [Omim][BF_4], [Bmim][BF_4], [Bmim][PF_6], [Emim][Tf_2N], [Emim][$EtSO_4$] and [Emim][SCN]. The performance, such as the coefficient of performance, *COP,* and circulation ratio *f,* along with the environmental temperature used as heat source were compared for these ILs based pairs and the conventional ones. This work on double-effect heat pumps with NH_3/ILs pairs shows that there is an optimum distribution ratio between the parallel flows and that some of the investigated mixtures have the potential to show a better performance than that of the traditional NH_3/H_2O pair in cooling and heating applications.

Selection and/or peer-review under responsibility of the organizers of the 12th IEA Heat Pump Conference 2017.

Keyworks: double-effect; absorption cycle; heat pump; ILs; NH_3

Nomenclature

COP	Coefficient of performance	-
C_p	Specific heat	$Jkg^{-1}K^{-1}$
DR	Distribution ratio	-
f	Circulation ratio	-
G	Parameters in NRTL model	-
h	Enthalpy	Jkg^{-1}
$\dot{m}$	Mass flow	kgs^{-1}
P	Pressure	Pa
$\dot{Q}$	Heat flow	W
T	Temperature	K
w	Mass fraction	$kgkg^{-1}$
x	Molar fraction	$molmol^{-1}$

Greek symbols

α , τ	Parameters in NRTL model	-
Δh	Enthalpy change	Jkg^{-1}
γ	Activity coefficient	-

Sub- and superscripts

0	Reference state
1 …18	State points
a	Absorber
c	Condenser
cooling	Cooling
e	Evaporator
hg	High pressure generator
hp	Heat pump
IL	Ionic liquid component
NH_3	ammonia component
mix	Mixing
r	Refrigerant
s	Solution
sat	Saturated
sol	Solution
t	Total

Abbreviations

ABS	Absorber
AHP	Absorption heat pump
CON	Condenser
DE	Double effect
EOS	Equation of state
EVA	Evaporator
HC	High pressure condenser
HC	Hydrocarbon
HFC	hydrofluorocarbons
HG	High pressure generator
HX	Heat exchanger
iHX	Intermediate heat exchanger
IL	Ionic liquid
LG	Low pressure generator
NRTL	Non-random two liquid
SE	Single effect
SHX	Solution heat exchanger
VLE	Vapor liquid equilibrium

1. Introduction

Absorption refrigeration and heat pump cycles, are drawing considerable attention because they can make use of the low-grade heat from the surroundings for the purpose of cooling and/or heating [1] [2]. Binary mixtures such as H_2O/LiBr, NH_3/H_2O have been widely used in absorption systems for decades, but many challenges do exist, such as crystallization possibilities of the H_2O/LiBr pair and the difficulty in separation of NH_3/H_2O pair [3]. Research to identify alternative absorbents which don't have these problems is most relevant [4].

Ionic liquids (ILs), as novel absorbents, have been attracting researchers for their potential roles in replacing water or aqueous solutions of LiBr in conventional absorption refrigeration and heat pump technology, because they hold strengths such as high boiling point, good affinity with refrigerants and high chemical and thermal stabilities [3]. In order to preselect promising ILs to be used in absorption systems, many researchers did performance prediction investigations, covering both experiment and simulation work. However due to the relatively high cost of ILs, experimental work [5]–[7] is up to now restricted to small scales and mainly based on H_2O/ILs pairs. The majority of the investigations were focused on performance predictions, in which the

frequently studied refrigerants include H_2O [8], [9], hydrocarbons (HCs) [10], hydrofluorocarbons (HFC) [11], [12], CO_2 [13] and NH_3 [14], [15]. However, all these researches were based on single-effect (SE) absorption systems. There are no publications that we are aware of concerning the topic of ILs in double-effect (DE) absorption systems.

Double-effect absorption heat pumps (DE-AHPs) can utilize high temperature heat input from concentrated solar power or process waste streams. It is possible to apply the working mixtures of IL with refrigerant in DE-AHP systems for maximum utilization of high temperature heat sources, for the IL mixtures will remain in liquid state under such operating conditions, while the current technology with LiBr-water mixtures may not [16]. Additionally, it is expected that higher energetic efficiencies will be obtained when optimized ionic liquid refrigerants mixtures will be used [17].

Since NH_3 based absorption systems hold strengths such as sub-zero degree applications and free of air infiltration [18], research using this natural refrigerant is most relevant. While reported works on this fluid on DE-AHPs are rare. In this work, we therefore intend to develop DE-AHPs in a parallel configuration using NH_3/ILs mixtures. Working fluids investigated here cover all the 9 NH_3/IL pairs for which their vapor-liquid equilibrium (VLE) data and ILs' heat capacity data have been reported. The operation ranges which are restricted by the VLE of each mixture will be first studied. Then a performance analysis will be carried out for the feasible working fluids. The optimum distribution ratio (*DR*) for each working fluid is also investigated.

2. Methodology

2.1 Cycle configuration

Fig 1 depicts a schematic of a DE-AHP system in parallel configuration. The main feature of the parallel DE-AHP cycle is that the strong solution (strong in refrigerant NH_3), pumped from the absorber (ABS), is divided into two parallel streams after being heated in the solution heat exchanger (SHX1). Two sub-streams are heated in two generators for generating refrigerant vapor. One of the sub-streams of the strong solution is heated in the high pressure generator (HG) by the external heat source at a high temperature. Superheated refrigerant vapor is generated there and then goes to the high pressure condenser (HC). In the HC, it releases the condensation heat which is utilized to heat the low pressure generator (LG). The other sub-stream of strong solution flows to the LG and is heated by this condensation heat to boil off the other stream of refrigerant vapor. The HC and LG are coupled in an intermediate heat exchanger (iHX). After the generation of refrigerant vapor, the two sub-streams of weak solution mix before they flow back to the ABS. The two streams of refrigerant vapor flow to the low pressure condenser (CON), rejecting the condensation heat to the surroundings (here cooling water). The sum of liquid refrigerant after CON passes through a throttle valve and the evaporator (EVA) to expand to a vapor state again before it is absorbed by the weak solution in ABS. The vaporization heat is extracted from the environmental heat source and absorption heat in released to the cooling water. An additional economizer (HX) is utilized to pre-heat the vapor refrigerant for the purpose of efficiency improvement.

Key state points of the solution are also illustrated qualitatively in both ln *P* -1/*T* and *h*-*w* diagrams in Fig. 2. The cycle 5-8-9-11a-11-13-5 shows the sub-stream passing the HG and cycle 5-7c-11b-11-13-5 represents the other one passing the LG. The mass flows of the two sub-streams of the solution can be quantified with the help of the distribution ratio *DR*, which is defined as the mass flow ratio of the sub-stream of the solution passing the HG to the total one.

$$DR = \frac{\dot{m}_{hgs}}{\dot{m}_{ts}} = \frac{\dot{m}_8}{\dot{m}_5} \tag{1}$$

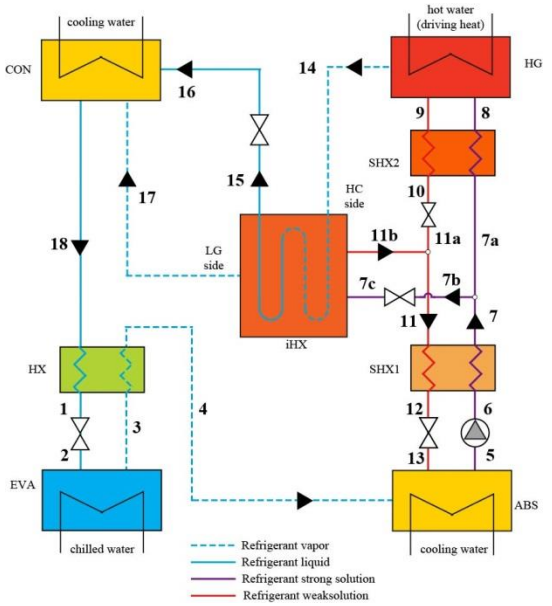

Fig. 1. Schematic diagram of a double-effect system absorption a parallel configuration

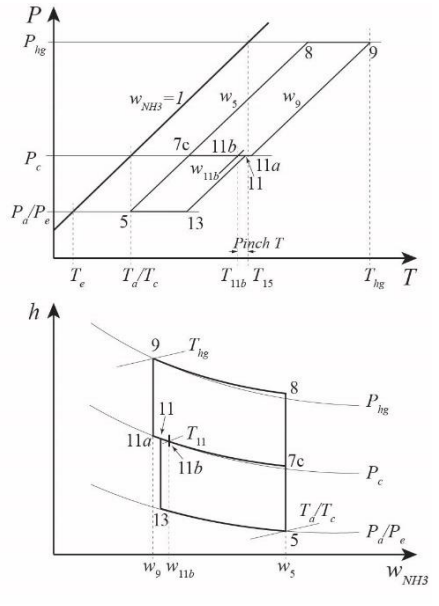

Fig. 2. The solution state points in ln*P*- -1/*T* in and h-w diagrams

2.2 Modelling methodology

In order to create an integrated model for the thermodynamic analysis of the DE-AHP system, several assumptions are made to simplify the calculations:

- The system operates in steady state.
- The operating pressures of absorber and evaporator are the same, and similarly the pressure of each generator is equal to its directly linked condenser.
- The refrigerant stream is saturated liquid or saturated vapor in the outlets of the two condensers and evaporator, respectively. The solution is in equilibrium state while leaving both generators. The solution leaving the absorber is subcooled with a subcooling of 3 K.
- For the heat exchangers, the pinch temperature of SHXs is assumed as 10 K. The pinch temperature of iHX is set to 5 K. The effectiveness of HX is assumed as 75 %.
- The heat losses, pressure losses and pumping work are neglected. Throttling is an isenthalpic process.

The calculation procedure for the whole system is illustrated in Fig. 3.

For each component, the energy, mass and species balances are taken into consideration for modelling. With the pressure-temperature-concentration information and enthalpy of each state point, which will be introduced in the next section, the rejected or absorbed heats $\dot{Q}_{hg}$, $\dot{Q}_c$, $\dot{Q}_e$ and $\dot{Q}_a$ could be obtained. Key performance parameters such as coefficient of performance, *COP,* for cooling and heating, are defined by,

$$COP_{cooling} = \frac{\dot{Q}_e}{\dot{Q}_{hg}} \tag{2}$$

$$COP_{hp} = \frac{\dot{Q}_a + \dot{Q}_c}{\dot{Q}_{hg}} \tag{3}$$

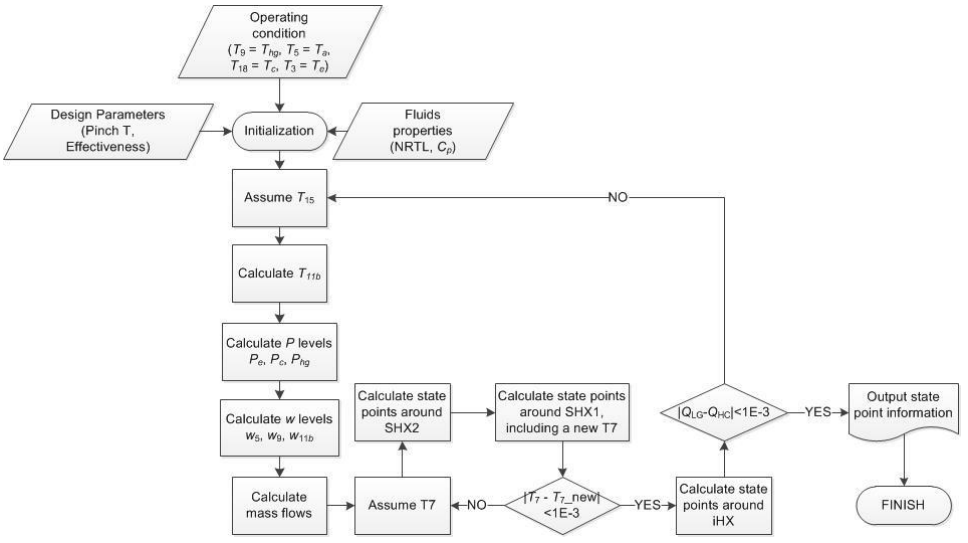

Fig. 3. Calculation procedure for the DE-AHP in a parallel configuration

The circulation ratio, *f,* which describes the mass flow ratio between the pumped solution stream and the pure refrigerant stream, can be obtained from

$$f = \frac{\dot{m}_{ts}}{\dot{m}_r} = \frac{1 - w_{13}}{w_5 - w_{13}} \tag{4}$$

2.3 Properties

2.3.1 Vapor liquid equilibrium for the NH_3/ILs binary solutions

Non-random two-liquid (NRTL) model for the prediction of vapor liquid equilibrium (VLE) of mixtures have been frequently reported in the literature, see for instance [19]. In this section only the details for the following steps of this paper will be discussed.

For the NH_3 / IL systems, due to the non-volatility of ILs, the equilibrium criterion is simplified as,

$$P = x_{NH_3} P_{NH_3}^{sat} \gamma_{NH_3} \tag{5}$$

here, $P_{NH_3}^{sat}$ can be obtained from Antoine equation. The activity coefficient γ_1 can be obtained by the NRTL activity coefficient model,

$$\ln \gamma_i = x_2^2 \left[\tau_{21} \left(\frac{G_{21}}{x_1 + x_2 G_{21}} \right)^2 + \frac{G_{12}\tau_{12}}{(x_2 + x_1 G_{12})^2} \right] \tag{6}$$

where,

$$G_{12} = \exp(-\alpha\tau_{12}) \quad G_{21} = \exp(-\alpha\tau_{21}) \tag{7}$$

$$\tau_{12} = \tau_{12}^{(0)} + \frac{\tau_{12}^{(1)}}{T} \qquad \tau_{21} = \tau_{21}^{(0)} + \frac{\tau_{21}^{(1)}}{T} \tag{8}$$

With the experimental vapor pressure data, the binary parameters α, $\tau_{12}^{(0)}$, $\tau_{12}^{(1)}$, $\tau_{21}^{(0)}$ and $\tau_{21}^{(1)}$ have been fitted and will allow for the determination of the operating concentrations in the next steps. The fitted results and accuracies can be found in [15].

2.3.2 Specific enthalpies of the refrigerant and mixtures

The specific enthalpy data of pure NH_3 are directly obtained from NIST's Refprop [20]. For solutions, the total specific enthalpies can be estimated using the following method, depending on its state,

For saturated solution at an equilibrium condition *T*, *P* and w_{NH3},

$$h\left(T,P,w_{NH_3}\right)=w_{NH_3}h_{NH_3}\left(T\right)+w_{IL}h_{IL}\left(T\right)+\Delta h_{mix}\left(T,P,w_{NH_3}\right) \tag{9}$$

where, the enthalpies of NH_3 and ILs are both chosen at their liquid states. And for the ILs, with the help of their pure heat capacities C_p^{IL},

$$h_{IL}\left(T\right)=h_0\left(T_0\right)+\int_{T_0}^{T}C_p^{IL}dT \tag{10}$$

The mixing enthalpy (excess enthalpy) Δh_{mix} can be estimated from methods based on the VLE data if experimental resources are not available. However, some researchers blamed the poor performance of these methods [21] and the authors' previous work showed that neglecting of Δh_{mix} does not significantly change the *COP* in a single-effect AHP [22]. For these reasons, in the following calculation, the mixing enthalpy will be neglected.

For subcooled solution at a condition *T*, *P* and w_{NH3}, the corresponding equilibrium temperature T_{sat} (at *P* and w_{NH3}) should be obtained first. Then the enthalpy can be expressed as,

$$h\left(T,P,w_{NH_3}\right)=h\left(T_{sat},P,w_{NH_3}\right)-\int_{T}^{T_{sat}}C_p^{sol}dT \tag{11}$$

where, the first term in the right side is the enthalpy of the corresponding saturated solution which can be obtained with Eq. 9, and the second one accounts for the subcooled effect by using the heat capacity of the solution C_p^{sol}.

The data of heat capacities of the solutions are rare for the NH_3/IL solutions [15]. In this study, the weighted average heat capacities of both components has been implemented to express C_p^{sol}.

$$C_p^{sol}\left(w_{NH_3}\right)=w_{NH_3}C_p^{NH_3}+\left(1-w_{NH_3}\right)C_p^{IL} \tag{12}$$

This treatment has been verified for H_2O/[Dmim]DMP with C_p^{sol} data in [8] showing that the relative deviation of the weighted average heat capacity is always smaller than 4%.

3. Results and discussion

3.1 Thermodynamic operation limits

In the generators, NH_3 concentration in the inlets should be greater than that in the outlet. This is a requirement that all working fluids must meet for proper operation of parallel DE-AHP systems. This statement is used as the thermodynamic criterion to evaluate the operating ranges of working fluids in certain applications.

The temperature of the HC outlet in the DE-AHP system, T_{15}, plays the role of determining the outlet concentrations of both generators. In the high pressure solution cycle, the pressure of the HG is the same as the saturated pressure of T_{15}. Thus together with T_{hg}, the HG outlet concentration w_9 can be determined. In the mid-pressure solution cycle, T_{11b} (obtained from T_{15} by subtracting the pinch temperature of iHX), along with the condenser pressure, defines the LG outlet concentration w_{11b}. Fig.4 shows the impact of T_{15} (the temperature of the CON outlet) on the outlet concentrations of the generators.

Making T_{15} higher, the pressure in HG, P_{hg} increases and consequently the outlet concentration w_9 in the HG comes closer to the inlet value, w_5. Thus T_{15} must be low enough to ensure $w_9 < w_5$. This can be used to find the

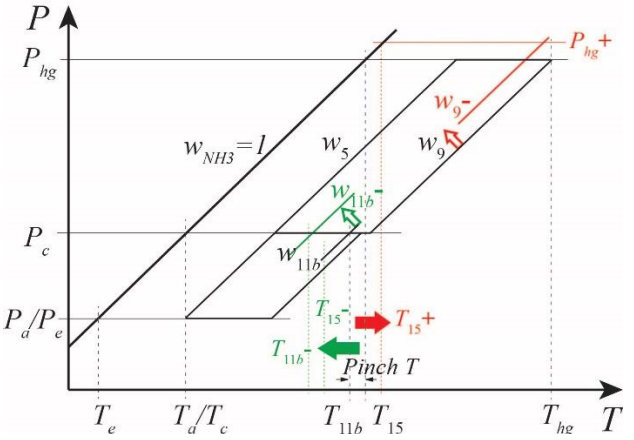

Fig. 4. Operation limits analysis of DE-AHP system.

maximum limit of T_{15}. Making T_{15} lower, taking the constrain imposed by the pinch temperature of the iHX, the outlet temperature of LG will also drop. This leads to a decrease of the outlet concentration of the LG, making it closer to LG's inlet concentration. Thus T_{15} should also be high enough to ensure $w_{11b} < w_5$. This can be used to identify the minimum value of T_{15}.

This analysis shows that T_{15} should be kept in a certain range to ensure a proper operation of the DE-AHP system. If all the external operating conditions such as T_e, T_c, T_a, T_{hg} are fixed, T_{15} will only be influenced by the different values of *DR* in terms of the energy balance of the iHX. A broad range of T_{15} implies a more flexible operating range and more options for the *DR*.

Thus, before predicting the performance of the DE-AHP systems, an analysis of the operation limits of the different working pair candidates is required.

Table 1 lists T_{15} ranges for the 9 NH_3/IL and NH_3/H_2O pairs for a cooling application with $T_{hg}/T_a/T_c/T_e$ = 175/30/40/10 ℃. Except for the pairs with [Emim][$EtSO_4$] or [Hmim][BF_4] (in red), most of the working pairs using ILs have relatively large operation ranges. Compared with H_2O's, NH_3 pairs with [Bmim][BF_4], [Emim][BF_4], [Emim][SCN] and [Mmim][DMP] have comparable ranges.

Table 1. T_{15} ranges for cooling operation ($T_{hg}/T_a/T_c/T_e$ = 175/30/40/10 ℃)

Absorbent	T15_min (℃)	T15_max (℃)	Range of T15 (K)
[Bmim][BF_4]	70.	121.	50.
[Bmim][PF_6]	72.	111.	39.
[Emim][BF_4]	70.	118.	48.
[Emim][$EtSO_4$]	72.	84.	13.
[Emim][SCN]	73.	120.	47.
[Emim][Tf_2N]	73.	112.	40.
[Hmim][BF_4]	88.	92.	4.
[Mmim][DMP]	67.	128.	61.

[Omim][BF_4]	76.	102.	26.
H_2O	69.	121.	52.

For a heating application, similar results are listed in Table 2. For the condition $T_{hg}/T_a/T_c/T_e$ = 175/45/45/10 ℃ most of the working pairs cannot operate since the required range of T_{15} is unrealistic (in red). The promising pairs which show operating ranges comparable to NH_3/H_2O include [Bmim][BF_4], [Emim][SCN] and [Mmim][DMP].

Table 2. T_{15} ranges for heating operation ($T_{hg}/T_a/T_c/T_e$ = 175/45/45/10 ℃)

Absorbent	T_{15}_min (℃)	T_{15}_max (℃)	Range of T_{15} [K]
[Bmim][BF_4]	95.	105.	9.
[Bmim][PF_6]	102.	87.	-14.
[Emim][BF_4]	97.	95.	-2.
[Emim][$EtSO_4$]	96.	67.	-29.
[Emim][SCN]	98.	107.	9.
[Emim][Tf_2N]	101.	91.	-9.
[Hmim][BF_4]	130.	70.	-59.
[Mmim][DMP]	91.	104.	12.
[Omim][BF_4]	111.	76.	-34.
H_2O	93.	107.	14.

3.2 Performance prediction for cooling applications

Based on the previous investigation of the operating ranges, the NH_3/ILs working pairs are selected for the theoretical study of the DE-AHP systems in a cooling application. The operating conditions of the system correspond to the conditions listed in Table 1.

The influence of the distribution ratio on the performance of the absorption refrigeration system has been investigated for each of the working pairs. As shown in Fig. 5, there is always a distribution ratio that gives the optimum *COP*. For most of the NH_3/ILs, the optimum *DR*s are around 0.5.

The performance of different working pairs is also presented in Fig. 5. At the optimum *DR*, the pairs with [Bmim][BF_4], [Emim][SCN] and [Mmim][DMP] have performance comparable to that of the NH_3/H_2O pair. The optimum *COP*s are around 1.3. In the current calculation for the NH_3/H_2O pair, the rectifier is not taken

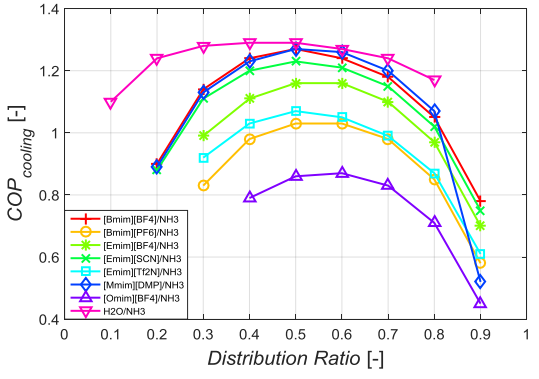

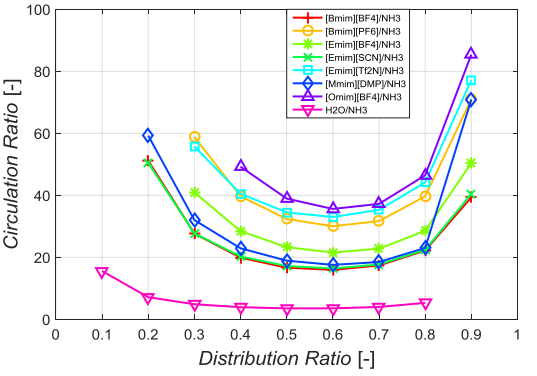

Fig. 5. Influence of *DR* on the *COP* for the selected NH_3/IL working pairs in a cooling application of DE-AHP

Fig. 6. Influence of *DR* on the *f* for the selected NH_3/IL working pairs in a cooling application of DE-AHP

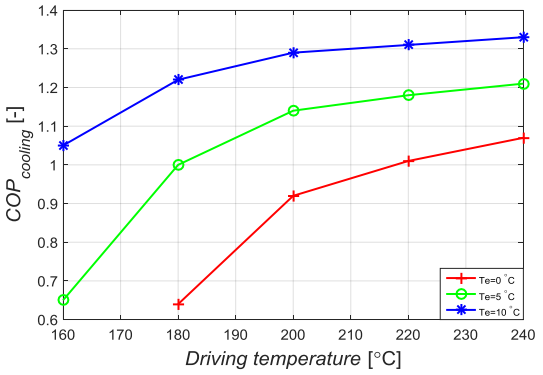

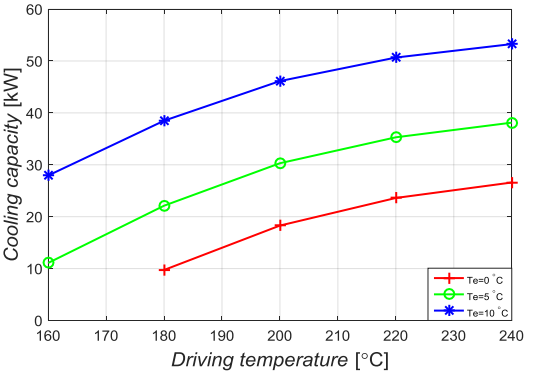

Fig. 7. Influence of T_{hg} on the *COP* of double effect refrigeration systems with NH_3/[Emim][SCN] pairs

Fig. 8. Influence of T_{hg} on cooling capacity of double effect refrigeration systems with NH_3/[Emim][SCN] pairs

into account. The $\dot{Q}_{hg}$ value of the system using NH_3/H_2O pair does not take the heat removed by the rectifier into account. In reality the generator requires additional heat to compensate for the heat removal of the rectifier. In practice this leads to a significant decrease of the *COP* [23], [24]. For the optimum *DR* conditions, the performance of parallel double-effect absorption systems using NH_3/IL pairs is expected to be higher than for systems which use NH_3/H_2O as working fluid.

The effect of different *DR* values and working pairs on the circulation ratio, *f*, is shown in Fig. 6. The optimum *DR* for *f* is still around 0.5 to 0.6. The previously mentioned 3 promising ILs show also relatively low *f* values compared with other ILs. However, the lowest *f* still applies for the NH_3/H_2O pair.

Additionally, the influence of the driving temperature, T_{hg}, on *COP* and cooling capacity has also been studied for the NH_3/[Emim][SCN] pair when the *DR* is taken as 0.5. The cooling capacities have been calculated based on a constant solution mass flow of 0.54 kg/s leaving the absorber.

In Fig. 7, as T_{hg} rises, the *COP* experiences an increase, but the increment becomes smaller at high temperature levels. The cooling capacity increases at an approximately linear trend with an increase of T_{hg} as shown in Fig. 8. The impact of the variation of the cooling temperature, T_e, on performance is also illustrated in Figs. 7 and 8. A lower cooling temperature leads to a lower *COP* and a lower cooling capacity.

3.3 Performance prediction for heating applications

Section 3.1 made clear that only a few NH_3/IL mixtures can operate under the proposed heating application conditions. It is also shown that the operating ranges for the feasible ILs are very limited. For this reason a slightly higher driving temperature, T_{hg}, is adopted in the further discussion: 200 ℃. The application temperatures (T_a and T_c) and environmental temperature (T_e) are maintained at 45 ℃ and 10 ℃, respectively.

The impact of *DR* on *COP* and *f* have been investigated for this heating application condition. Fig. 9 shows that the optimum *DR* is 0.6 for the 3 pairs containing IL. Among them, [Bmim][BF_4] and [Emim][SCN] pairs perform the best. However their optimum *COPs* are below 2.0. The mixtures NH_3/H_2O perform better then the NH_3/IL mixtures. Similar results apply for *f* as illustrated in Fig. 10.

The performance of NH_3/[Emim][SCN] pair in a DE-AHP system has also studied as shown in Figs. 11 and 12. As T_{hg} increases, the *COP* and heating capacity both increase. By decreasing the environmental temperature, T_e, the *COP* and heating capacity both decrease.

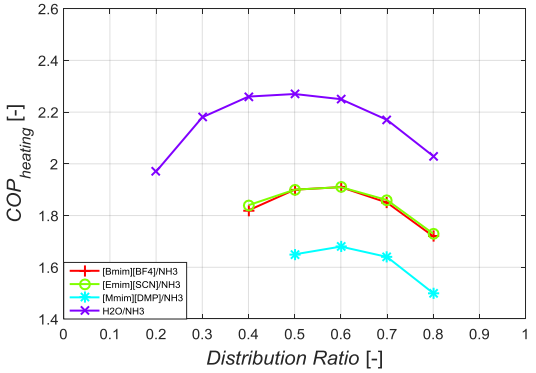

Fig. 9. Influence of *DR* on the *COP* for the selected NH_3/IL working pairs in a heating application of DE-AHP

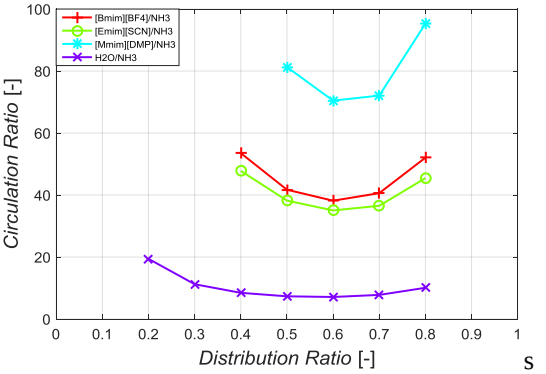

Fig. 10. Influence of *DR* on the *CR* for the selected NH_3/IL working pairs in a heating application of DE-AHP

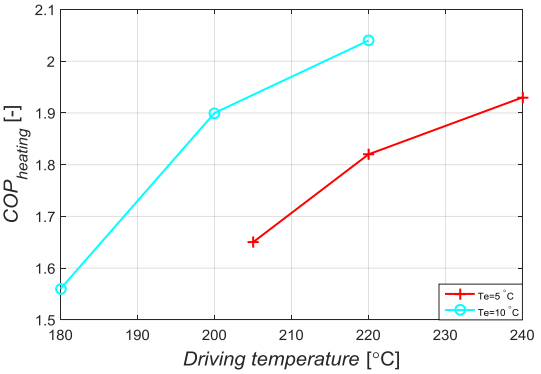

Fig. 11. Influence of T_{hg} on the *COP* of a DE-AHP system with NH_3/[Emim][SCN] pairs

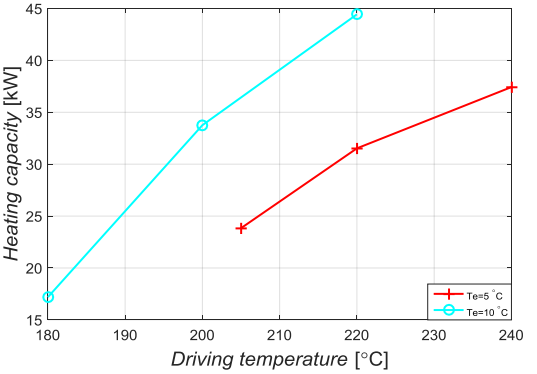

Fig. 12. Influence of T_{hg} on heating capacity of DE-AHP system with NH_3/[Emim][SCN] pairs

4. Conclusions

This paper discusses NH_3/IL working pairs in double effect absorption heat pump systems.

- A thermodynamic model has been proposed to describe the parallel configuration DE-AHP with NH_3-ILs as working fluids.
- An analysis of the thermodynamic limits of operation added with performance prediction revealed that the best performing ammonia pairs are those with [Bmim][BF_4], [Emim][SCN] and [Mmim][DMP].
- The optimum of system is around 0.5.
- At the optimum distribution ratio, NH_3/ILs have the potential to show a better performance than that of the traditional NH_3/H_2O pair in cooling applications in DE-AHP systems.

- The effects of driving temperature and surrounding temperature on the performance have been investigated. NH_3-IL systems will perform better at higher heating medium temperatures.

Acknowledgements

The authors acknowledge support from the China Scholarship Council for this research.

References

[1] D. S. Kim and C. A. Infante Ferreira, "Solar refrigeration options – a state-of-the-art review," *Int. J. Refrig.*, vol. 31, no. 1, pp. 3–15, Jan. 2008.

[2] A. Zaltash, E. A. Vineyard, D. T. Rizy, and R. L. Linkous, "Integration of Microturbine with single-effect exhaust-driven absorption chiller and solid wheel desiccant system," in *International Sorption Heat Pump Conference*, 2005, pp. 1–6.

[3] D. Zheng, L. Dong, W. Huang, X. Wu, and N. Nie, "A review of imidazolium ionic liquids research and development towards working pair of absorption cycle," *Renew. Sustain. Energy Rev.*, vol. 37, pp. 47–68, Sep. 2014.

[4] J. Sun, L. Fu, and S. Zhang, "A review of working fluids of absorption cycles," *Renew. Sustain. Energy Rev.*, vol. 16, no. 4, pp. 1899–1906, May 2012.

[5] S. Kim, Y. J. Kim, Y. K. Joshi, A. G. Fedorov, and P. a. Kohl, "Absorption Heat Pump/Refrigeration System Utilizing Ionic Liquid and Hydrofluorocarbon Refrigerants," *J. Electron. Packag.*, vol. 134, no. 3, pp. 15–30, 2012.

[6] M. Radspieler and C. Schweigler, "Experimental investigation of ionic liquid emim EtSO4 as solvent in a single-effect cycle with adiabatic absorption and desorption," in *Proc. of the Int. Sorption Heat Pump Conf.*, 2011, pp. 125–134.

[7] M.-C. Schneider, R. Schneider, O. Zehnacker, O. Buchin, F. Cudok, A. Kühn, T. Meyer, F. Ziegler, and M. Seiler, "Ionic liquids: new-high performance working fluids for absorption chillers and heat pumps," in *Proc. of the Int. Sorption Heat Pump Conf.*, 2011, pp. 95–106.

[8] L. Dong, D. Zheng, N. Nie, and Y. Li, "Performance prediction of absorption refrigeration cycle based on the measurements of vapor pressure and heat capacity of H2O+[DMIM]DMP system," *Appl. Energy*, vol. 98, pp. 326–332, Oct. 2012.

[9] E.-S. Abumandour, F. Mutelet, and D. Alonso, "Performance of an absorption heat transformer using new working binary systems composed of {ionic liquid and water}," *Appl. Therm. Eng.*, vol. 94, pp. 579–589, Feb. 2016.

[10] W. Chen and S. Liang, "Thermodynamic analysis of absorption heat transformers using [mmim]DMP/H2O and [mmim]DMP/CH3OH as working fluids," *Appl. Therm. Eng.*, vol. 99, pp. 846–856, 2016.

[11] D. S. Ayou, M. R. Currás, D. Salavera, J. García, J. C. Bruno, and A. Coronas, "Performance analysis of absorption heat transformer cycles using ionic liquids based on imidazolium cation as absorbents with 2,2,2-trifluoroethanol as refrigerant," *Energy Convers. Manag.*, vol. 84, pp. 512–523, Aug. 2014.

[12] M. B. Shiflett and A. Yokozeki, "Absorption Cycle Utilizing Ionic Liquid As Working Fluid," US 20060197053Al, 2006.

[13] W. Cai, M. Sen, and S. Paolucci, "Dynamic Modeling of an Absorption Refrigeration System Using Ionic Liquids," in *Proceedings of 2007 ASME International Mechanical Engineering Congress and Exposition*, 2007, pp. 227–236.

[14] A. Yokozeki and M. B. Shiflett, "Vapor–liquid equilibria of ammonia+ionic liquid mixtures," *Appl. Energy*, vol. 84, no. 12, pp. 1258–1273, Dec. 2007.
[15] M. Wang and C. A. Infante Ferreira, "Performance prediction of single-effect absorption heat pump cycles using ionic liquids," in *Proc. of the 12th IIR Gustav Lorentzen Natural Working Fluids Conference*, 2016.
[16] L. Garousi Farshi, S. M. Seyed Mahmoudi, and M. A. Rosen, "Analysis of crystallization risk in double effect absorption refrigeration systems," *Appl. Therm. Eng.*, vol. 31, no. 10, pp. 1712–1717, 2011.
[17] S. C. Kaushik and A. Arora, "Energy and exergy analysis of single effect and series flow double effect water-lithium bromide absorption refrigeration systems," *Int. J. Refrig.*, vol. 32, no. 6, pp. 1247–1258, 2009.
[18] C. Vasilescu and C. Infante Ferreira, "Solar driven double-effect absorption cycles for sub-zero temperatures," *Int. J. Refrig.*, vol. 39, pp. 86–94, 2014.
[19] A. A. Kiss and C. A. Infante Ferreira, *Heat Pumps in Chemical Process Industry*. CRC Press, 2016.
[20] E. W. Lemmon, M. L. Huber, and M. O. McLinden, "NIST reference fluid thermodynamic and transport properties–REFPROP." U.S. Department of Commerce, 2013.
[21] M. B. Shiflett and A. Yokozeki, "Solubility and diffusivity of hydrofluorocarbons in room-temperature ionic liquids," *AIChE J.*, vol. 52, no. 3, pp. 1205–1219, Mar. 2006.
[22] M. Wang and C. A. Infante Ferreira, "Absorption heat pump cycle with NH3 - ionic liquid working pairs," *In-review*, 2016.
[23] H. T. Chua, H. K. Toh, and K. C. Ng, "Thermodynamic modeling of an ammonia–water absorption chiller," *Int. J. Refrig.*, vol. 25, no. 7, pp. 896–906, Nov. 2002.
[24] A. Yokozeki, "Theoretical performances of various refrigerant–absorbent pairs in a vapor-absorption refrigeration cycle by the use of equations of state," *Appl. Energy*, vol. 80, no. 4, pp. 383–399, Apr. 2005.